**Proceedings of the 23rd National Heat and Mass Transfer Conference and
1st International ISHMT-ASTFE Heat and Mass Transfer Conference
IHMTC2015
17-20 December, 2015, Thiruvananthapuram, India**

Paper No. IHMTC2015- 862

LATENT HEAT THERMAL ENERGY STORAGE IN A HEATED SEMI-CYLINDRICAL CAVITY: EXPERIMENTAL RESULTS AND NUMERICAL VALIDATION

Amit Saraswat
Department of Mechanical Engineering
Indian Institute of Technology Kanpur
Kanpur 208016, India
Email: amitsar@iitk.ac.in

Ankit Verma
Department of Mechanical Engineering
Indian Institute of Technology Kanpur
Kanpur 208016, India
Email: verank@iitk.ac.in

Sameer Khandekar
Department of Mechanical Engineering
Indian Institute of Technology Kanpur
Kanpur 208016, India
Email: samkhan@iitk.ac.in

Malay K Das
Department of Mechanical Engineering
Indian Institute of Technology Kanpur
Kanpur 208016, India
Email: mkdas@iitk.ac.in

ABSTRACT

Thermal energy storage in general, and phase-change materials (PCMs) in particular, have been a major topic of research for the last 30 years. Because of their favorable thermo-dynamical characteristics, such as high density, specific heat and latent heat of fusion, PCMs are usually employed as working fluids for thermal storage. However, low thermal conductivities of organic PCMs have posed a continuous challenge in deployment of the technology.

This study focuses on experimental investigation of the melting process of industrial grade paraffin wax inside a semi-cylindrical enclosure with a heating strip attached axially along the center and its validation with the numerical results. During the study, the solid-liquid interface location, the liquid flow patterns, spatial variation of temperature over time and thermal maps of the system were recorded. For numerical simulation of the system, open source library OpenFOAM® was used in order to numerically solve Navier-Stokes and energy equations in the considered system. The quantitative comparisons between experimental results and numerical simulations were carried out to validate the results obtained. This experimental setup and the numerical algorithm are being used as a starting point in the design of future PCM storage systems; study presently underway. With due validation, the model can be used to design thermal storage systems for electrical sub-stations.

Keywords: Phase-change materials, thermal energy storage, latent heat, convection, transport phenomena

NOMENCLATURE

A	surface area (m^2)
C_p	specific heat (J/kg-K)
k	thermal conductivity (W/m-K)
h	heat transfer coefficient (W/m^2-K)
Re	Reynold's number (-)
Nu	Nusselt number (-)
Pr	Prandtl number (-)
T	temperature at any point in domain (K)
t	time (s)
I	current (A)
m	mass (kg)
R	resistance (Ω)
V	voltage (V)
E	energy (J)
h_{fg}	latent heat of fusion (J/kg)
μ	dynamic viscosity (Pa-s)
ν	kinematic viscosity (m^2/s)
ρ	density (kg/m^3)

INTRODUCTION

The ongoing and rapid increase in the economic development worldwide is accompanied by a strong demand for an uninterrupted supply of energy. Conventional energy resources, primarily fossil fuels, have uncertainties concerning sustained stable supply and pricing associated with them. Additionally, they also have led to increase in the level of greenhouse emissions. The increasing concerns about climate change and environmental issues have led to demands of conserving energy through development of energy efficient systems.

In spite of obvious advantages, renewable energy also has a major limitation i.e. the reliability of supply. Renewable energy often relies on weather pattern, solar incidence etc. When these resources are temporarily unavailable, the generation capacity gets directly affected. This makes the renewable energy sources unpredictable and inconsistent. By adopting a responsive, robust and effective energy storage approach, the variable and indeterminable gap existing between the supply and demand of the different types of renewable energy can be eliminated. To maintain grid security levels, a suitable solution is to integrate it with energy storage devices.

Thermal energy storage, or thermal storage, is an efficient available energy storage technology that provides a suitable solution to this problem and caters to energy demand through energy redistribution. [1-4] In thermal energy storage systems, energy in the form of heat or cold can be placed in a storage medium for a particular duration and can be retrieved from the same location for later usage. Amongst all thermal heat storage techniques, latent heat thermal storage stands out due to its inherent ability to provide high energy storage densities with low temperature changes [5-7].

The latent heat storage can be accomplished through phase-change from solid to solid, solid to gas, liquid to gas or solid to liquid. However, for all practical purposes, only the solid to liquid change is used. Liquid to gas phase-change is not put into use as the thermal storage requires large volumes to store the materials when in their gas phase, even though they have a higher heat of transformation than solid to liquid transitions. Solid to solid phase changes are also unfavorable as they are too slow and have a low heat of transformation. Out of the two main Latent heat thermal energy storage methods, Phase Change Material (PCM) thermal energy storage is preferred because phase-change materials have better thermo physical properties, exhibit good phase-change characteristics during charging and discharging cycles, have higher energy storage densities and have the ability to store heat at the temperature at which phase transition of phase-change material takes place. Thus, phase-change materials offer higher storage capacity and storage efficiencies (75% - 90%). The organic phase-change materials usually used typically have lower melting temperatures, and have an advantage of congruent melting. However, phase-change materials, generally used for Latent heat thermal energy storage typically have low thermal conductivity in solid state which limits the energy storage capacity of the storage system. Thus, the conductivity enhancement of phase-change materials is one of the most difficult challenges posed in thermal energy storage [8-9].

The present paper studies the challenges posed by low thermal conductivity of PCMs. Experimental and numerical simulations of convection dominated phase-change in a semi-cylindrical cavity filled with paraffin wax with an attached heater strip is performed. The numerical method used is the enthalpy-porosity technique extended by a continuous enthalpy function which allows the solution of the energy conservation equation without updating. This extended method given by Rosler et al. [10] is compared with the measurements of gallium melting in a rectangular cavity. Preliminary measurements of technical grade paraffin in the vertical semi-cylindrical test rig are compared with simulations, which shows a good match.

EXPERIMENTAL SETUP AND PROCEDURE

The setup has a semi-cylindrical enclosure as shown in Fig. 1 and 2 that consists of two stainless steel concentric half cylinders, with diameters 11 cm and 15 cm respectively, thickness 1 cm and a common length 30 cm. The inner and outer cylinders are mounted on a stainless steel frame of thickness 2 cm via welding and a rectangular window of the dimensions of the inner cylinder (diameter x length) is carved out. This window is adjusted to aid the visualization of the process in the inner cylinder. The half cylinders are sealed on either side via stainless steel plates having thickness of 10 mm. The plates are sealed to the concentric cylinders by welding. The inner half cylinder is used to store the Paraffin Wax, the volume of this inner cylinder being referred to as the melt pool. The annular region between the inner and the outer cylinder is evacuated to maintain vacuum to ensure minimum heat loss. The leak tight window is then fitted with a 10 mm thick transparent poly-acrylic sheet that aids visualization of the melt pool and acts as an insulator ensuring minimum heat loss. A stainless steel electric heating strip, 4 mm wide and 100 micron thick, with an electrical impedance of 1.2 Ω is embedded axially along the vertical center line of the acrylic sheet. This heater strip is then connected via a regulator to a 60 V, 50 A DC supply.

In the melt pool, six thermocouples are suspended at different locations. One of them, is exclusively used to monitor the temperature of the heater strip while the other five are appointed at different (r, Θ, z) in the cylindrical coordinate system. They measure the temperature of the paraffin wax at different locations and at different times.

Some additional liquid wax is always maintained in a wax reservoir present at the top of the cylinder by an electric heating element attached to it. The height of wax in the reservoir is matched with the maximum height of wax in the melt pool, which ensures that the melt pool is completely filled with wax at all times. This ensures that the volume of wax in the cylinder remains constant and compensates for the phase-change induced density variation of wax.

The organic PCM used in this setup is Paraffin Wax (CAS No: 8002-74-2). The observed properties of the wax used for the experiment at 21° C are:

- melting point : 60°C
- latent heat of fusion (h_{fg}) : 220 J/g
- thermal conductivity (k) : 0.3414 W/m-K
- thermal diffusivity (α) : 0.09716 mm^2/s
- specific heat of solid (C_p) : 3.5146 kJ/kg-K

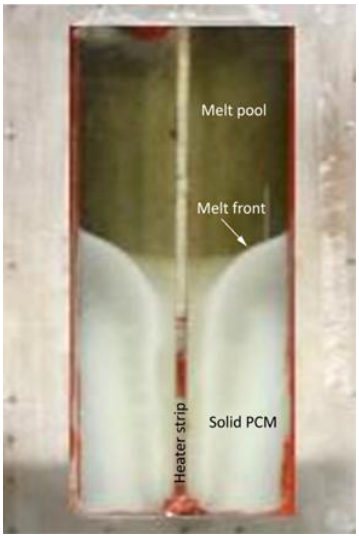

FIGURE 1: Experimental setup: Heated semi-cylindrical cavity (front view seen from the camera).

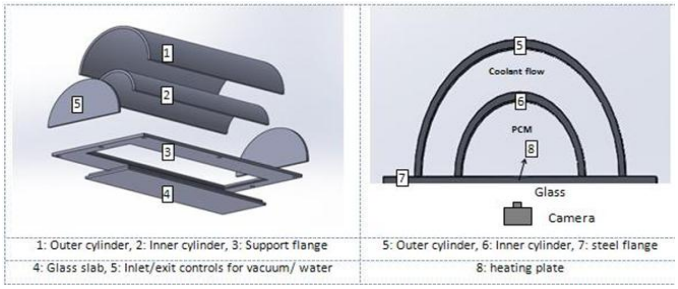

FIGURE 2: Exploded view of the experimental setup showing the half-cylindrical PCM cavity; Dirichlet boundary condition is maintained between outer shell #1 and inner shell #2; PCM material is stored in volume 6. Heating stripe is designated as 8.

The experimental procedure gives an overview of the way the organic PCM (Paraffin wax in this case) stored in the semi-cylindrical cavity behaves when a constant heat flux boundary condition is applied to the strip heater. The results shed light on the effects of natural convection, melting and convection phenomena, visualization and general overview of the time required during such a transport process.

During the experiments, the wax in the semi-cylindrical enclosure is melted by passing constant current through the heater strip. The current is increased to a steady value of 7.5A. It is ensured that the constant heat flux boundary condition is maintained at all later times through the circuit i.e. the current in the circuit remains steady. As the wax melts, the melting front is visually recorded continuously (front view, as shown in Figure 1) over the time duration of melting. These images are then fed into an image processing code on MATLAB® which then tracks the melt front at each pixel and a definite shape is obtained for validation with numerical results.

The temperatures recorded by the thermocouples are used for understanding the melting phenomenon. The results of the numerical simulations are then validated with those obtained experimentally.

NUMERICAL MODEL

The numerical simulations performed in this paper are made under the following assumptions:

- The simulation domain is three dimensional.
- The Boussinesq approximations is valid
- The PCM is incompressible and its density can be considered constant, except for the buoyancy source term.

Consequently, the employed solid liquid model is based on the following continuum equations of the conservation of mass, momentum and energy [11],

$$\frac{\partial \rho}{\partial t} + \nabla.(\rho \mathbf{U}) = 0 \tag{1.1}$$

$$\frac{\partial \rho \mathbf{U}}{\partial t} + \nabla.(\rho \mathbf{U}\mathbf{U}) = -\nabla p + \nabla.(\mu \nabla \mathbf{U}) + \mathrm{S}_U \tag{1.2}$$

$$\frac{\partial (\rho C_p T)}{\partial t} + \nabla.(\rho \mathbf{U} C_p T) = \nabla.(k \nabla T) + \mathrm{S}_T \tag{1.3}$$

Here ρ is the fluid density, $\mathbf{U}$ is the velocity vector, t time, p pressure, μ dynamic viscosity, C_p specific heat constant, T temperature, and k thermal conductivity. Additionally, S_U and S_T are momentum and energy source terms, respectively. These source terms are explained below.

Momentum source and sink

The contribution of the term S_U is two-fold. First, the temperature difference creates a density difference, which results in the buoyancy force in the direction of the gravity vector. Second, the velocity field has to vanish in the solid, thus there has to be momentum sink which decelerates the flow in the solid. Accordingly, S_U reads,

$$\mathrm{S}_U = S_u + S_d = \rho g \hat{\boldsymbol{e}}_y \beta (T - T_{ref}) + A\mathbf{U} \tag{1.4}$$

where,

$$A = -\frac{C(1-f_l)}{f_l^3 + e_0} \tag{1.5}$$

The first term (the thermal buoyancy) makes use of the Boussinesq approximation, where g is the gravitational acceleration constant, $\hat{\boldsymbol{e}}_y$ is a unit vector pointing in the positive y direction, and β is the thermal expansion coefficient. The latter (the momentum sink) depends on the liquid fraction f_l, which is zero in the solid and unity in the liquid. The multiplier C is a constant which is chosen to be large enough, whereas e_0 is a small constant to avoid the division by zero when the liquid fraction f_l, is zero in the solid. In the solid, s_d acts as a dominant sink in the momentum equation, thus enforcing the zero velocity field. On the other hand, in the liquid zone, the above term vanishes and a velocity field is obtained using the other terms in the momentum equation.

Energy source term

The energy source term accounts for the evolution of the latent heat during phase-change. The latent heat is absorbed during melting process, whereas it is released during solidification. This term reads,

$$S_T = -\left[\frac{\partial \rho \Delta H}{\partial t} + \nabla.(\rho \mathbf{U} \Delta H)\right] \tag{1.6}$$

The latent heat ΔH is released or absorbed when the material undergoes a phase-change. It changes from zero in the solid to the maximum that equals the phase-change latent heat L in the liquid. For an isothermal phase-change, the convection of latent heat vanishes. For non-isothermal phase-change, the amount of latent heat is, in general, a function of the temperature in the interval.

Implementation of S_T makes use of the source term linearization technique, where the non-linearities are accounted for through iterations after transforming the term into the following linear form:

$$S_T = S_P T + S_C \tag{1.7}$$

Eq. 1.6 can be rewritten as,

$$S_T = -\frac{\partial\left(\rho f_l L\right)}{\partial t} = -\rho L \frac{\partial f_l}{\partial T}\frac{\partial T}{\partial t} \tag{1.8}$$

where f_l is the liquid fraction and L the phase-change latent heat. The convective term is omitted for simplicity. For a linear profile of latent heat in the melting interval, the liquid fraction f_l reads,

$$f_l = \begin{cases} 0 & if\ T \le T_s \\ \dfrac{T - T_s}{T_l - T_s} & if\ \ T_s \le T_l \\ 1 & if\ \ T \ge T_l \end{cases} \tag{1.9}$$

The coupling between the liquid fraction and the energy conservation equation requires an iterative solution procedure, updating the liquid fraction every iterative sweep. Application of a continuous liquid fraction would allow its direct substitution into the energy conservation equation. Hence, as is common in heat transfer applications, we describe the liquid fraction function using an error function given by,

$$f_l = 0.5.\mathrm{erf}\left(\frac{4(T - T_m)}{(T_l - T_s)}\right) + 0.5 \tag{1.10}$$

where, the melting temperature T_m is the arithmetic mean between T_l and T_s.The introduced energy equation is no function of the liquid fraction f_l anymore. Thus, standard solvers can be applied for solving the energy equation.
The introduced model was implemented in the open source computational fluid dynamics software OpenFOAM®. It is a linux based C++ framework consisting of fluid flow and heat transfer solvers. The PIMPLE (PISO-SIMPLE) algorithm for numerical solution is used for the transient simulations.

RESULTS AND ANALYSIS

Melting of gallium in a rectangular cavity

The gallium test case is a benchmark problem to evaluate the numerical model for solid/liquid phase-change process. Brent et al [12] compared their results with an experimental analysis performed by Gau and Viskanta [13]. The same test case is used to validate the current model.

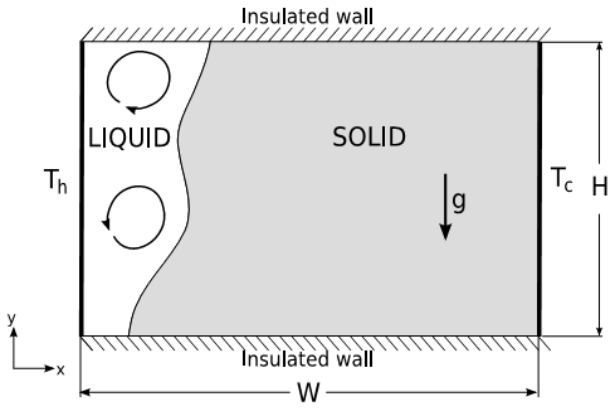

FIGURE 3: Computational domain of gallium test case.

The rectangular cavity consists of heated left wall and cold right wall with adiabatic top and bottom boundaries.

The boundary conditions are: T_h = 38°C, T_c = 28.3°C, with the gallium at an initial temperature of 28.3°C. Figure 3 illustrates the simulation domain based on the experiments of Gau and Viskanta [8]. The physical properties of gallium are tabulated in Table 1.

The domain size is 88.9 mm x 63.6 mm and it is divided into 42 x 32 hexahedral numerical cells.

Table 1 Thermophysical properties of gallium

Density, ρ	6093 kg/m^3
Volumetric thermal expansion coefficient of liquid, β	1.2 x 10^{-4} -
Thermal conductivity, k	32.0 W/mK
Melting point, T_m	29.78 °C
Latent heat of fusion, L	80160 J/kg
Specific heat capacity, C_p	381.5 J/kg-K
Dynamic viscosity, μ	1.81x10^{-3} kg/m-s

Figure 4 shows the moving solid/liquid boundary determined in the experiments by Gau and Viskanta [8] compared with the numerical model used in this paper. The comparison shows that the extended enthalpy-porosity method with continuous liquid fraction is capable to simulate convection dominated melting process. The simulated phase front matches the results of the experiment.

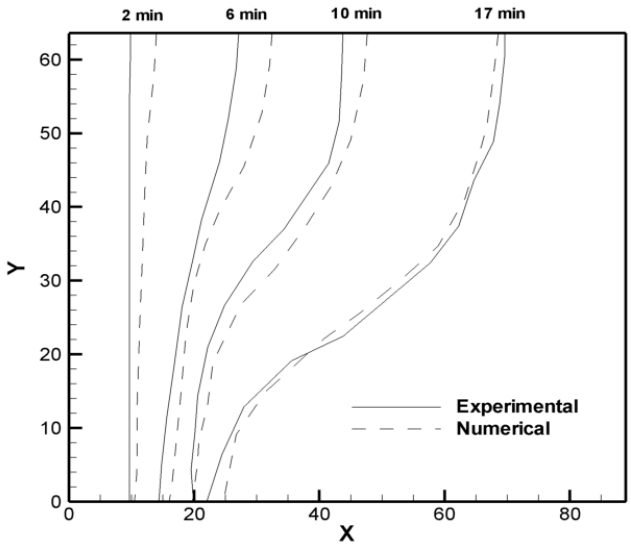

FIGURE 4: Comparison of interface of experimental and numerical study.

The slight discrepancies to the experiment can be explained by the three-dimensional effects in the test enclosure and the assumption of temperature independent physical properties in the simulation.

Melting of paraffin wax in a semi cylindrical cavity

The actual time for melting the paraffin wax during the experiment was observed to be nearly 17 hours which contrasts sharply with the expected theoretical time of 1.6 hours, based on net energy required. This is because despite high storage capacity, the thermal conductivity of the material is so low (0.3414 W/m-K) that with a line source in a cylindrical system, the material takes nearly 8X more time to reach the stage of melting than its theoretical possibility. Also, the rise of natural convection further lowers the dissipation of heat in the system and leads to compounding of effects, which increases the melting time.

The rise of convection currents leads to poor dissipation of heat in the system. The effect tends to increase, as more and more material in the pool melts into the liquid phase. Thus, the time required to melt per unit volume of paraffin wax increases as melting of the wax progresses.

The temperature-time dependence plot recorded by the thermocouples located at various locations in the melt pool shows that the melting temperature of 60°C is achieved quickly on the thermocouple with highest z coordinate of 27.5 cm from the base of the melt pool, whereas the subsequent progression for melting temperature becomes slower due to rise of convection currents and super-heating of the molten liquid. The variation of temperature over time is recorded spatially by one of the thermocouple in the system, as shown in Figure 5.

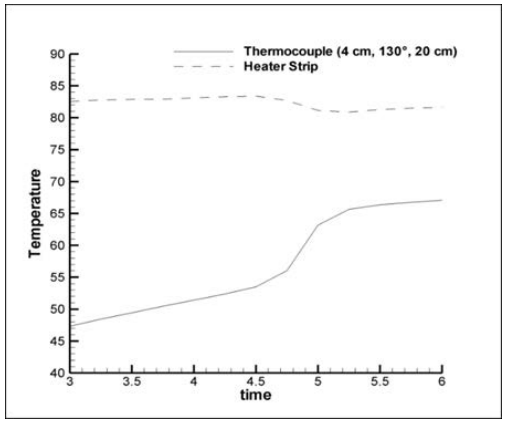

FIGURE 5: Experimental temperature variation with time for the heater strip and thermocouple installed at cylindrical coordinates 4 cm, 130°, 20 cm taking origin at the bottom of heater strip.

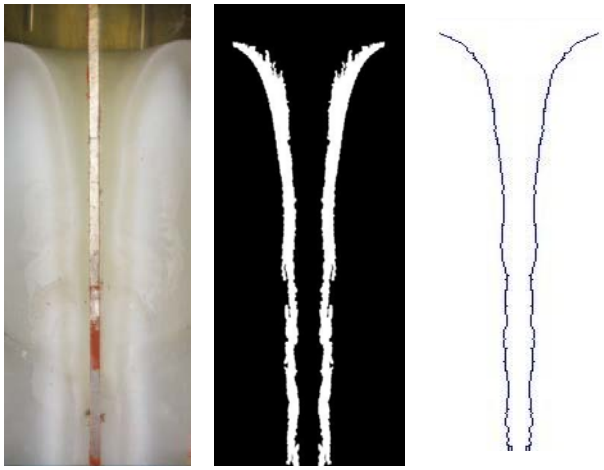

(a) t = 80 min

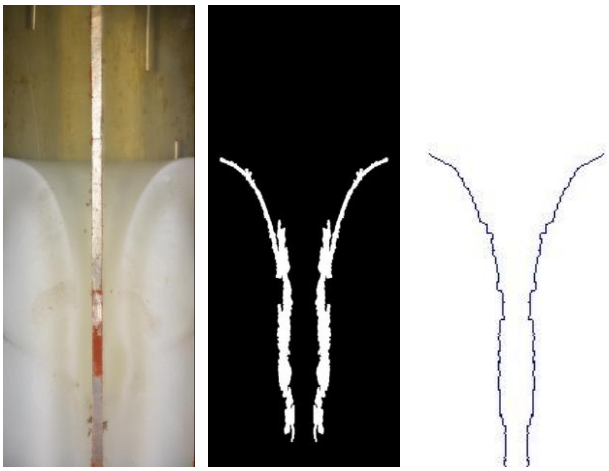

(b) t = 180 min

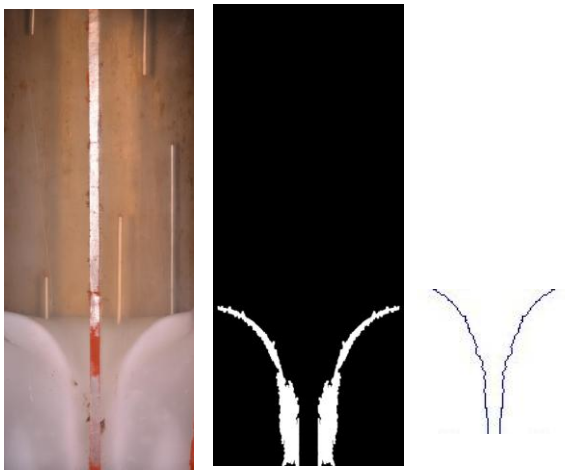

(c) t = 490 min

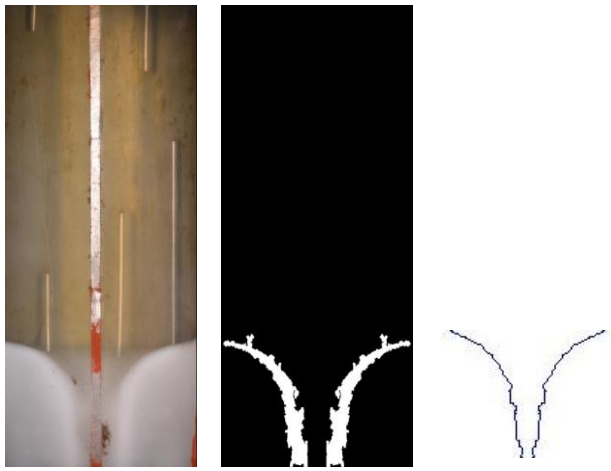

(d) t = 790 min

FIGURE 6: Melt fronts, their obtained plots and contour plot at various instants of time.

The melt profile captured every 10 minutes through the high resolution camera, are processed using a MATLAB code. The code possesses the images to quantitatively plot the melt fronts at various instants of time by converting each pixel from RGB to grey scale by calculating average value of red, blue and green coordinates at each location. Then, those pixels with average value within a 5 point range value of all the Red, Blue and Green coordinates of the same pixel are turned white. This leads to separation of the solid phase from the liquid-phase. Later, the contour of the solid-phase is plotted by extending it by five points in each direction and subtracting the original white solid pool from the same. This data is then numerically fed into MATLAB® to obtain quantitative values of X vs. Y for plotting the profile of the melt front.

Selected melt fronts at various instants of time, their obtained plots and the contour at various points in time obtained using MATLAB are as shown below in Figure 6 (a)-Figure 6 (d).

Natural convection currents are observed in melt pool and isotropic melting does not occur. Lower rise in temperature is observed post melting of some solid portion due to convective heat transfer and interplay of solid-liquid thermo physical properties. The heat storage in the melt pool was largely successful with a maintained heat pool of over five hours.

The computational domain for the setup is shown in Figure 7. The boundary and initial conditions used in the simulations are elaborated below

Boundary Conditions

Fixed Walls: No slip condition $\mathbf{U} = \mathbf{0}$, zero heat flux

$$\frac{dT}{dn} = 0$$

Heater Strip: No slip condition $\mathbf{U} = \mathbf{0}$, constant heat flux

$$\frac{dT}{dn} = \text{constant}$$

Initial Condition: Zero velocity throughout $\mathbf{U} = \mathbf{0}$, Constant temperature $T = T_0 < T_1$

The simulated results at different times are shown in Figure 8. The simulated results show a qualitative match with the experimental results. Some discrepancies are because of incomplete congruence of the experimental and numerical simulation conditions. The thermophysical data are adopted from the available experimental results [1]. The temperature dependent properties of paraffin wax have also not been taken into account in the simulation which can lead to some mismatch.

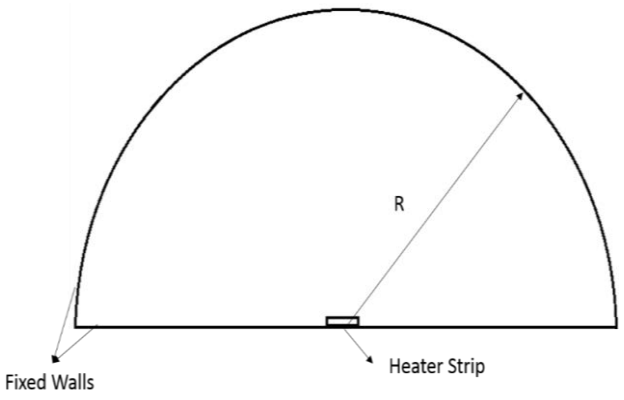

FIGURE 7: Computational domain for semi-cylindrical cavity (radius = R), showing the thin heater strip.

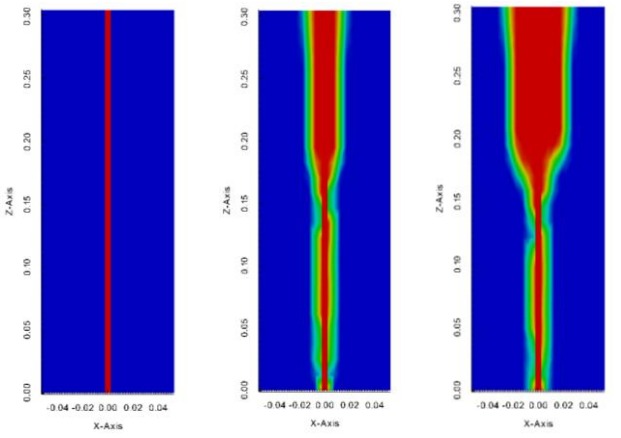

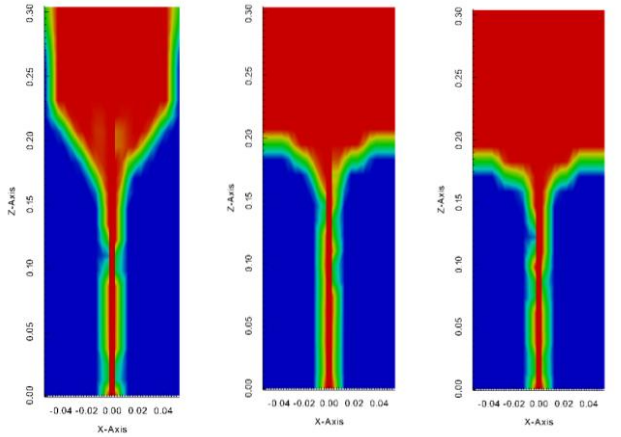

FIGURE 8: Transient simulation results for paraffin wax in semi-cylindrical cavity (OpenFOAM®).

SUMMARY AND CONCLUSIONS

It is observed that melting characteristics of Organic PCMs in melt pool shows qualitative coherency with numerical simulations on OpenFoam®. The melting process is severely affected by their low thermal conductivity and generation of natural convection currents in the melt pool, which further lower down the rise in temperature post melting due to interplay of solid/liquid thermo-physical properties and convective heat transfer. Understanding transport phenomena under such melting and cooling regimes will help design efficient thermal storage systems. It is clear that some technique to resolve this incongruent and slow melting need to be devised. In this direction, passive elements for enhancing the diffusive heat transfer are useful; implementation work of such enhancement technique is in progress.

REFERENCES

[1] Kemink, R.G., Sparrow, E.M., Heat transfer coefficients for melting about a vertical cylinder with or without subcooling and for open or closed containment, International Journal of Heat Mass Transfer, 24 (10) 1699–1710 (1981).

[2] Himran, S., Suwono A., Mansoori G.A., Characterization of alkanes and paraffin waxes for application as phase-change energy storage medium, Energy Sources 16 (1) 117–128 (1994).

[3] Cho, K, Choi, S.H., Thermal characteristics of a paraffin in a spherical capsule during freezing and melting processes, International Journal of Heat and Mass Transfer, 43, 3183-3196 (2000).

[4] Assis, E., Katsman, L., Ziskind, G., Letan, R., Numerical and experimental study of melting in spherical shell, International Journal of Heat and Mass Transfer, 50, 1790-1804 (2007).

[5] Kalaiselvam, S., Veerappan, M., Arul A.A, Iniyan, S. Experimental and analytical investigation of solidification and melting characteristics of PCMs inside cylindrical encapsulation, International Journal of Thermal Sciences, 47(7), 858-874 2008.

[6] Sharma A., Tyagi, V.V., Chen, R., Buddhi, D., Review on thermal energy storage with phase-change materials and applications, Renewable and Sustainable Energy Reviews, 13, 318–345 (2009).

[7] Petrone, G. Cammarata G., Simulation of PCM melting process in a differentially heated enclosure, Proc. 2012 COMSOL Conference in Milan (2012).

[8] Shmueli, H., Ziskind, G., Letan, R. Melting in vertical cylinder tube: numerical investigation and comparison with experiments, International Journal of Heat and Mass Transfer, 53, 4082-4091 (2010).

[9] Hosseini, M.J., Ranjba, A.A, Sedighi, K., Rahimi M. , A combined experimental and computational study on the melting behavior of medium temperature phase change storage material inside shell and tube heat exchanger, International Communications in Heat and Mass Transfer, 39, 1416-1424 (2012).

[10] Rosler, F., Bruggemann, D., Shell and tube type latent heat thermal energy storage: Numerical analysis and comparison with experiments, Heat Mass Transfer, 47, 1027-1033 (2011).

[11] Saldi, Z.S., Marangoni driven free surface flows in liquid weld pools, Ph.D. Thesis, TU Delft (2012).

[12] Brent, A., Voller, V., Reid, K., Enthalpy-porosity technique for modeling convection-diffusion phase-change: Application to the melting of pure metal, Numerical Heat Transfer - B, 13, 297-318 (1988).

[13] Gau, C., Viskanta, R., Melting and solidification of a pure metal on a vertical wall, Journal of Heat Transfer, 108, 174-181 (1986).